Figures and figure supplements

Insights into herpesvirus assembly from the structure of the pUL7:pUL51 complex

Benjamin G Butt *et al*

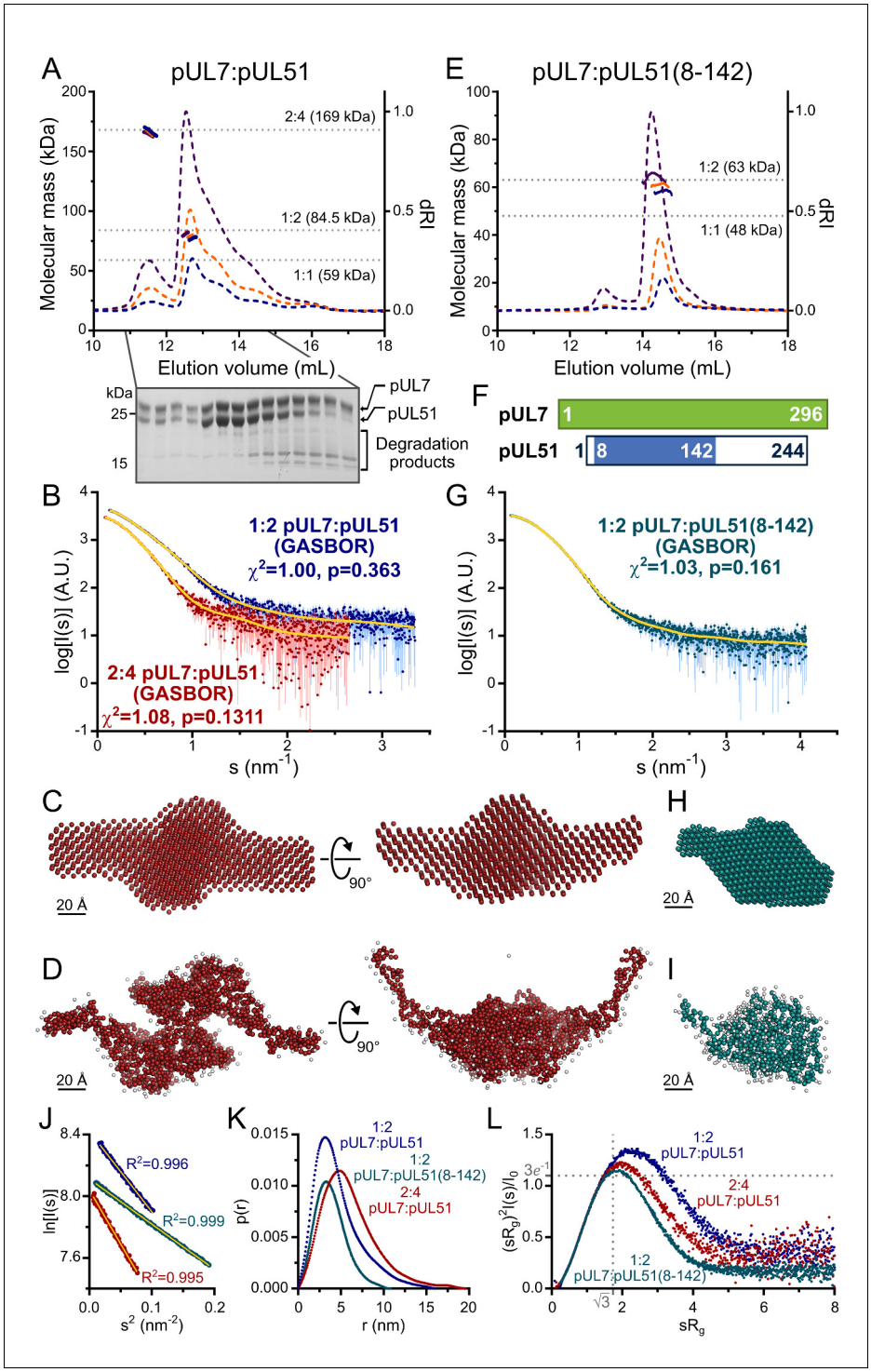

Figure 1. HSV-1 pUL7:pUL51 forms a 1:2 heterotrimeric complex in solution. (**A**) SEC-MALS analysis of recombinant full-length pUL7:pUL51 complex. Weight-averaged molecular masses (colored solid lines) are shown across the elution profiles (normalized differential refractive index, dRI, colored dashed lines) for samples injected at 2.4, 4.9 and 9.7 mg/mL (blue, orange and purple, respectively). The expected molecular masses for 1:1, 1:2 and 2:4 pUL7:pUL51 complexes are shown as dotted horizontal lines. (**B**) Averaged SAXS profiles through SEC elution peaks corresponding to 1:2 (blue) and 2:4 (red) complexes of pUL7:pUL51. Fits of representative GASBOR *ab initio* dummy-residue models to the scattering curves for each complex are shown in yellow. χ^2, fit quality. p, Correlation Map (CorMap) *P*-value of systematic deviations between the model fit and scattering data (61). (**C**) Refined

Figure 1 continued on next page

Figure 1 continued

DAMMIN dummy-atom model reconstruction of the 2:4 pUL7:pUL51 complex, shown in two orthogonal orientations. (**D**) Representative GASBOR dummy-residue model of the 2:4 pUL7:pUL51 complex, shown in two orthogonal orientations. This model comprises an anti-parallel dimer of heterotrimers, although we note that parallel dimers are also consistent with the scattering data. (**E**) SEC-MALS of pUL7:pUL51(8-142) complex. Elution profiles and molecular masses are shown as in (**A**) for recombinant pUL7:pUL51(8–142) injected at 0.6, 1.1 and 3.9 mg/mL (blue, orange and purple, respectively). (**F**) Schematic representation of pUL7 and pUL51. (**G**) Averaged SEC-SAXS profile through pUL7:pUL51(8–142) elution peak. Fit of a representative GASBOR *ab initio* dummy-residue model to the scattering curve is shown in yellow. (**H**) Refined DAMMIN dummy-atom model reconstruction of pUL7:pUL51(8–142) complex. (**I**) Representative GASBOR dummy-residue model of pUL7:pUL51(8-142). (**J**) Plot of the Guinier region ($sR_g < 1.3$) for SAXS profiles shown in (**B**) and (**G**). The fit to the Guinier equation (yellow) is linear for each curve, as expected for aggregate-free systems. (**K**) p(r) vs r profiles for SAXS profiles shown in (**B**) and (**G**). (**L**) Dimensionless Kratky plot of SAXS profiles shown in (**B**) and (**G**). The expected maximum of the plot for a compact globular domain that conforms to the Guinier approximation is shown ($sR_g = \sqrt{3}$, $(sR_g)^2 I(s)/I_0 = 3e^{-1}$, grey dotted lines).

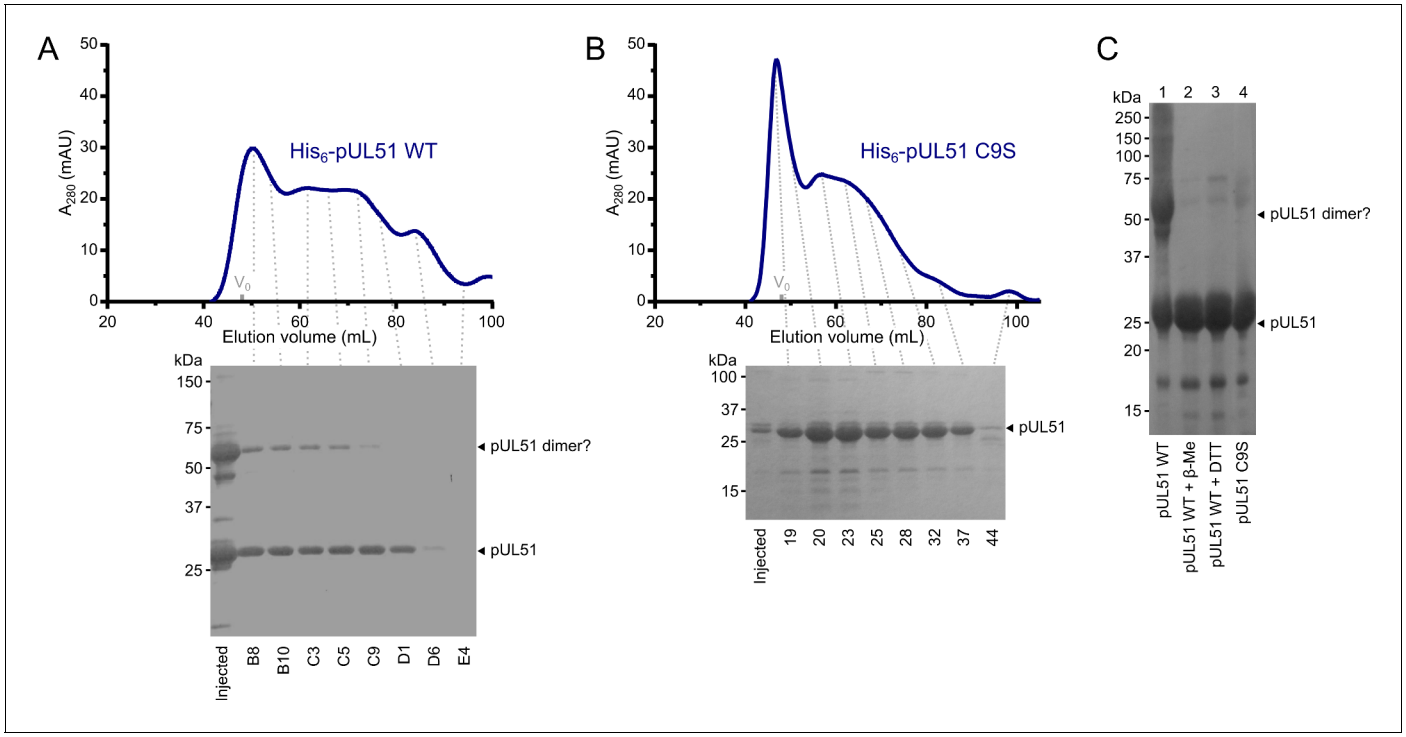

Figure 1—figure supplement 1. HSV-1 pUL51 forms large soluble aggregates when purified in isolation. (**A, B**) SEC elution profiles of (**A**) His_6-tagged wild-type pUL51 and (**B**) His_6-tagged pUL51 where Cys9 was substituted with serine (C9S). Proteins were injected onto an S200 16/600 column (GE Healthcare) equilibrated in 20 mM Tris (pH 7.5), 200 mM NaCl, 1 mM DTT. Both proteins have extended elution profiles with peaks near the column void volume (V_0), consistent with their forming large soluble aggregates. Coomassie-stained SDS-PAGE analysis of eluted SEC fractions are shown beneath each chromatogram. Note that there is a higher molecular weight band in (**A**), consistent with the presence of an SDS-resistant pUL51 dimer, despite the presence of 1 mM DTT in the SEC buffer and 2 mM DTT in the SDS-PAGE loading buffer. (**C**) Purified His_6-tagged wild-type pUL51 was subjected to SDS-PAGE either without additional treatment (*lane 1*) or following incubation with 50 mM β-mercaptoethanol (*lane 2*) or 50 mM DTT (*lane 3*). Comparison with the His_6-tagged pUL51 C9S mutant (*lane 4*) confirms that Cys9, the residue that becomes palmitoylated in mammalian cells (***Nozawa et al., 2003***), mediates disulfide bond mediated dimerization of recombinant wild-type pUL51. C9S substituted pUL51 (or truncations thereof) was thus used for all subsequent experiments with purified proteins.

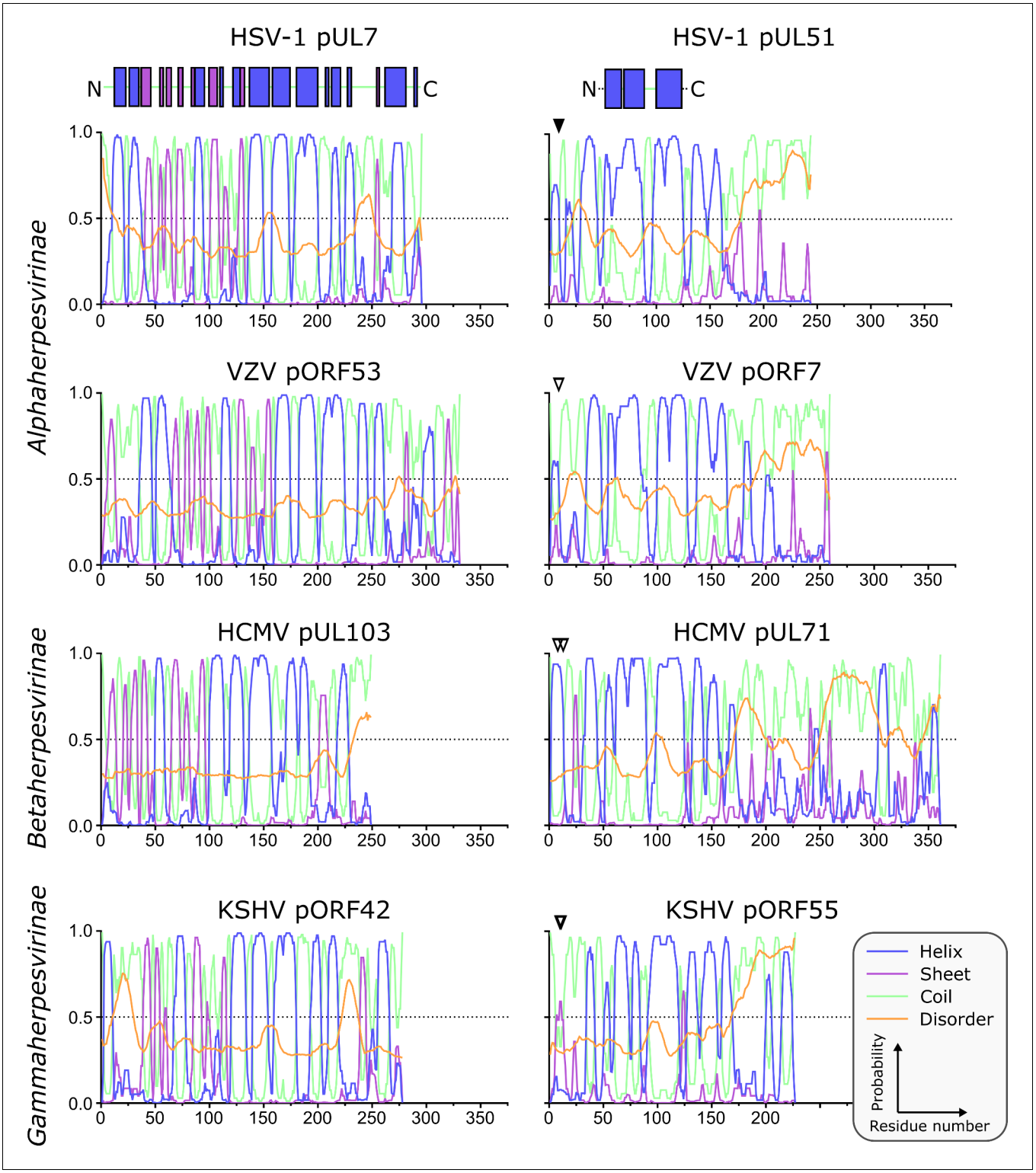

Figure 1—figure supplement 2. Predicted secondary structure of pUL7 and pUL51 homologues from representative human α-, β- and γ-herpesviruses. Analyses of amino acid sequences were performed as described in *Materials and Methods*. Per-residue probabilities of forming α-helix (blue), β-sheet (purple) or coil (green) are shown, as is the probability of disorder (orange). Residues that are known (solid triangles) or predicted (empty triangles) to be palmitoylated are marked: Cys9 of HSV-1 pUL51, Cys9 of VZV pORF7, Cys8 and Cys13 of HCMV pUL71, Cys10 and Cys11 of KSHV pORF55. Regions of pUL7 and pUL51 α-helix and β-sheet observed in the pUL7:pUL51(8–142) core heterodimer structure are shown above the predictions as boxes. The predicted pUL7 and pUL51 secondary structural elements are largely conserved across herpesvirus families, although the first two helices of pUL7 are

Figure 1—figure supplement 2 continued on next page

Figure 1—figure supplement 2 continued

not conserved in β-herpesviruses like HCMV. Additionally, the C-terminal regions of pUL51 homologues vary in length, although in all herpesvirus families they are predicted to be largely unstructured.

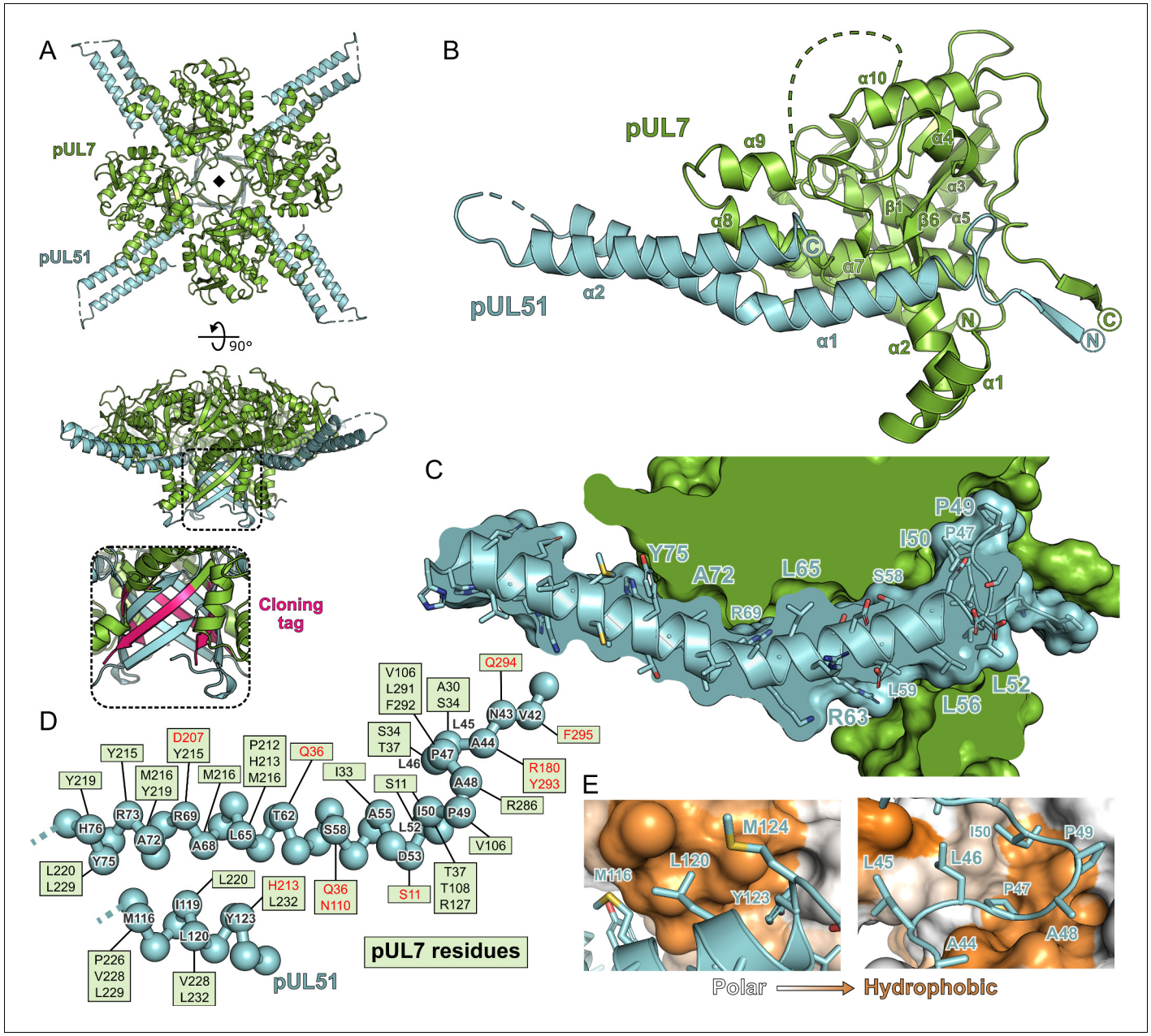

Figure 2. Structure of pUL7 in complex with pUL51. (**A**) Hetero-octamer of pUL7 and pUL51(8–142) observed in the crystallographic asymmetric unit. pUL7 and pUL51 are shown as green and cyan ribbons, respectively, in two orthogonal orientations. Inset shows residues arising from the pUL7 cloning tag (pink) that form an eight-stranded β-barrel with residues from pUL51. (**B**) Core heterodimer of pUL7 (residues 11–296) and pUL51 (residues 41–125). Selected secondary structure elements are labelled. (**C**) 'Cut-through' molecular surface representation of pUL7 (green) showing the intimate interaction interface with the hydrophobic loop and helix α1 of pUL51 (cyan). pUL51 side chains are shown as sticks. (**D**) Molecular interactions between pUL51 (cyan) and pUL7 (boxed residue names). Hydrophobic and hydrogen bond interactions are in black and red typeface, respectively. (**E**) Molecular surface representation of pUL7, colored by residue hydrophobicity from *white* (polar) to *orange* (hydrophobic). pUL51 is represented as a cyan ribbon with selected side chains shown.

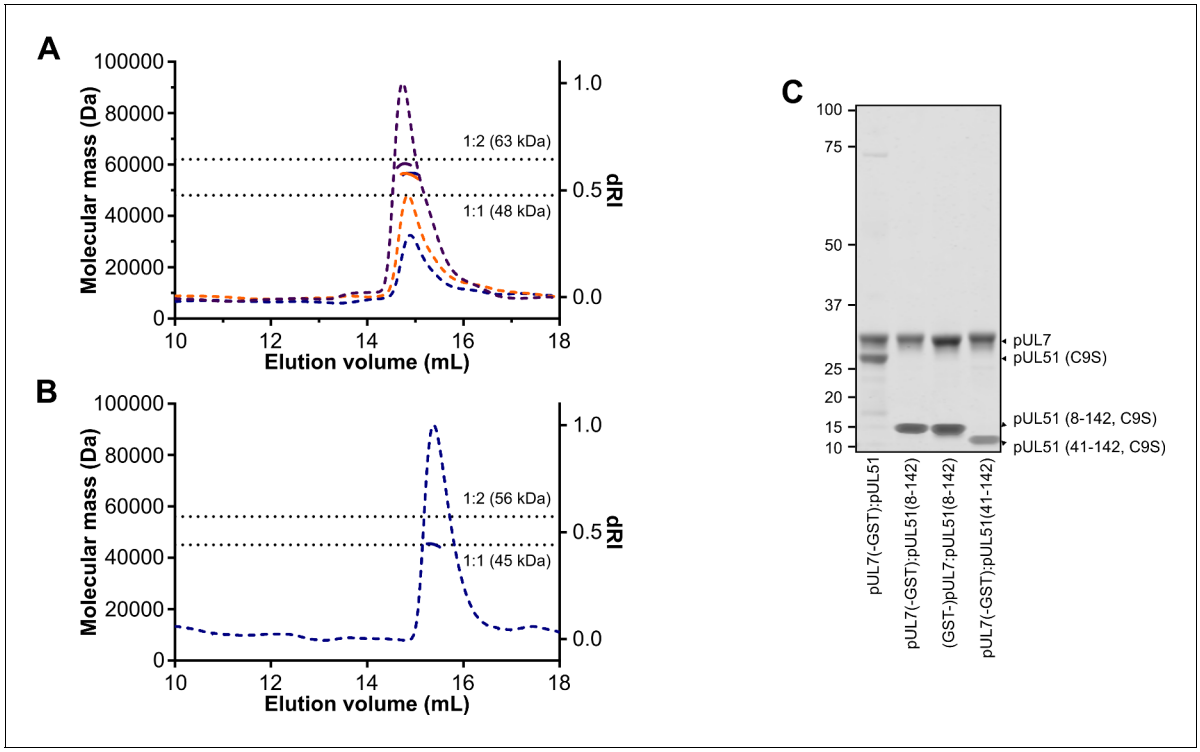

Figure 2—figure supplement 1. SEC-MALS of truncated pUL7:pUL51 complexes. (**A, B**) SEC elution profiles (differential refractive index, dashed lines) and weight-averaged molecular masses across the elution peaks (solid lines) are shown. (**A**) SEC-MALS of pUL7:pUL51(8–142) where pUL7 had been purified using an N-terminal GST tag that was subsequently removed using human rhinovirus 3C protease. Observed mass for the pUL7:pUL51(8–142) complex was 57.4 ± 2.2 kDa, compared with a theoretical mass of 62.7 kDa for a 1:2 heterotrimer. Samples were injected onto the column at 0.3 mg/mL (blue), 0.5 mg/mL (orange) and 1 mg/mL (purple). (**B**) SEC-MALS of pUL7:pUL51(41–142), injected onto the column at 0.3 mg/mL. The observed mass was 45.1 kDa, compared to a theoretical mass of 44.8 kDa for a 1:1 heterodimer (**C**) Coomassie-stained SDS-PAGE analysis of samples used for SEC-MALS analysis in (**A**), (**B**) and ***Figure 2***. The GST purification tag was cleaved from all samples used for SEC-MALS, the pUL7 protein having been tagged at the N or C terminus during the initial purification steps as shown.

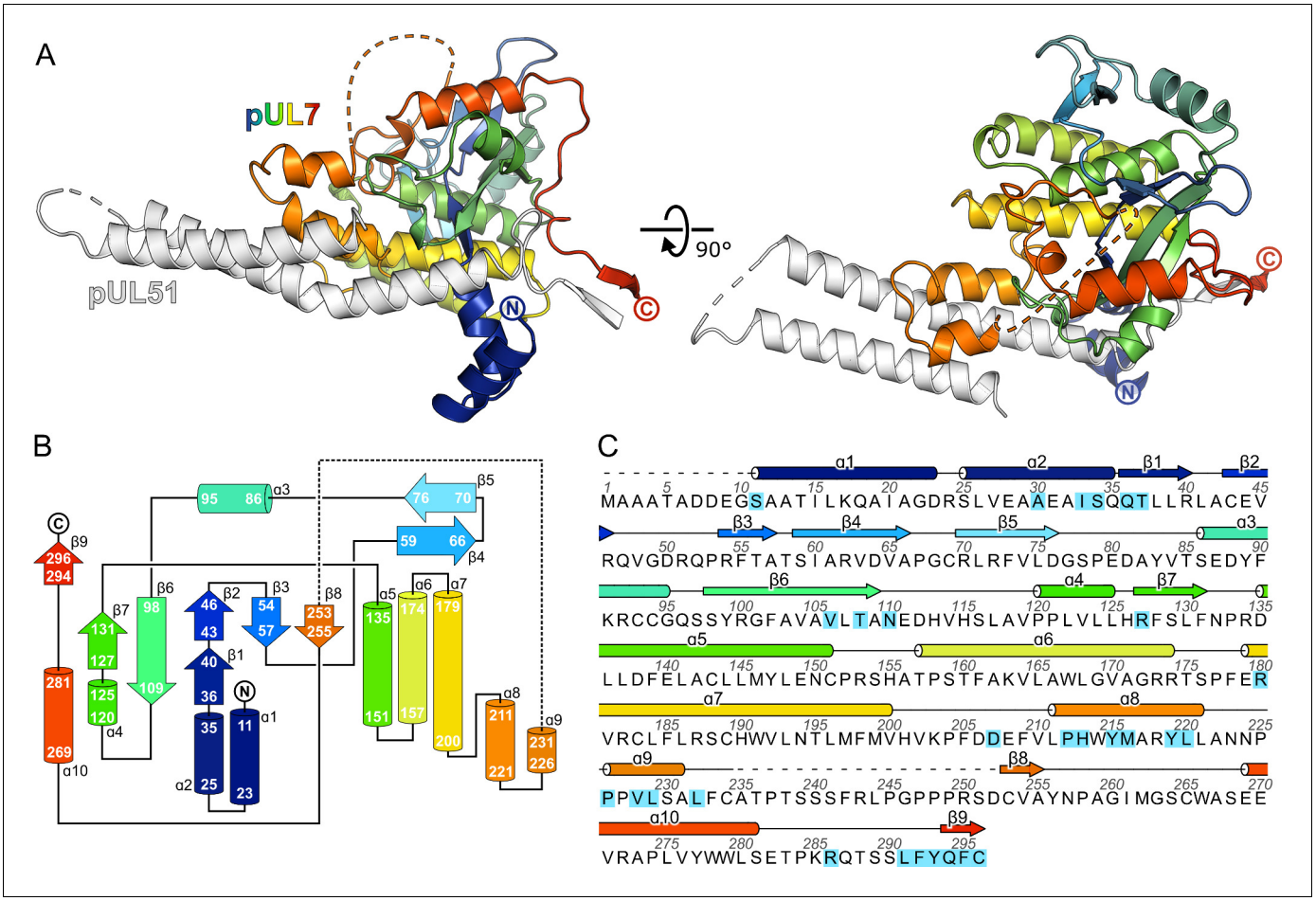

Figure 2—figure supplement 2. The CUSTARD fold of pUL7. (**A**) Structure of pUL7:pUL51(8–142) core heterodimer is shown as ribbons, with pUL51 colored white and pUL7 colored from blue (residue 11) to red (residue 296). Two orthogonal views are shown. (**B**) Schematic diagram of the topology of pUL7. (**C**) HSV-1 pUL7 sequence, with secondary structure shown above. Residues that interact with pUL51 are highlighted in cyan.

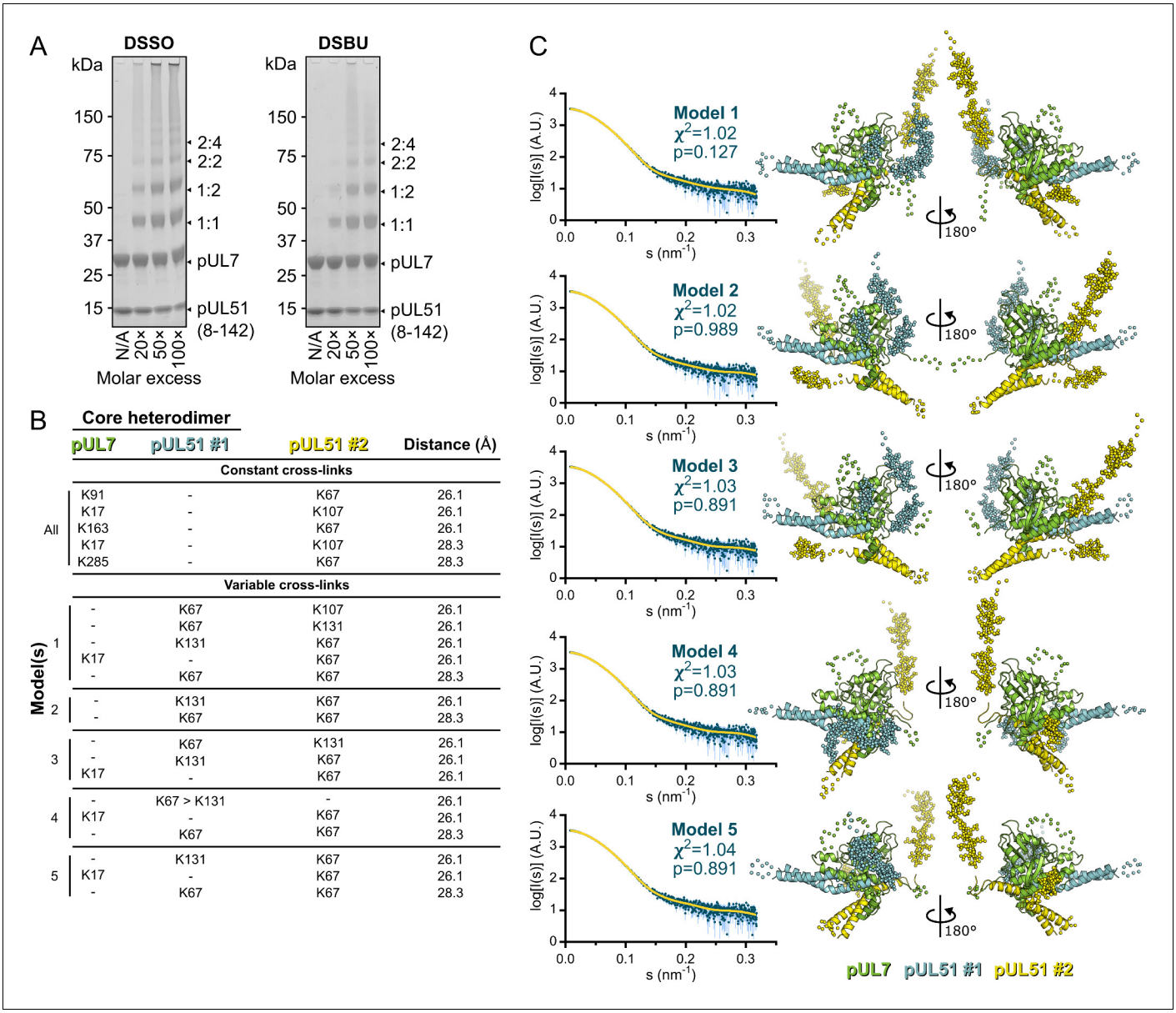

Figure 2—figure supplement 3. Cross-linking mass spectrometry analysis and pseudo-atomic modelling of the pUL7:pUL51(8–142) solution heterotrimer. (**A**) Coomassie-stained SDS-PAGE analysis of purified pUL7:pUL51(8–142) following 30 min incubation at room temperature with varying molar excesses of the cross-linking agents DSSO (left) or DSBU (right). Theoretical migration of proteins corresponding to pUL7, pUL51(8–142), and 1:1, 1:2, 2:2 or 2:4 complexes thereof, are indicated. (**B**) Cross-linking restraints used for pseudo-atomic modelling of the pUL7:pUL51(8–142) heterotrimer. Restraints used for all models ('constant cross-links') and permuted restraints ('variable cross-links') that were used for the five best-fit (lowest χ^2) models are shown. (**C**) The five best pseudo-atomic models (lowest χ^2) generated by fitting to the pUL7:pUL51(8–142) SAXS profile as described in *Materials and Methods* using the restraints shown in (**B**). The core heterodimer of pUL7 (residues 11–234 and 253–296; green) and pUL51 (residues 41–89 and 96–125; #1, cyan) and the additional molecule of pUL51 (residues 41–89 and 96–125; #2, yellow) are shown as ribbons (right). Additional regions modelled using I-TASSER or CORAL are shown as spheres. The fit of the computed scattering (yellow) to the pUL7:pUL51(8–142) SAXS profile (aqua) is shown for each model (left), as are reduced χ^2 and CorMap *P*-values (***Franke et al., 2015***; ***Petoukhov et al., 2012***).

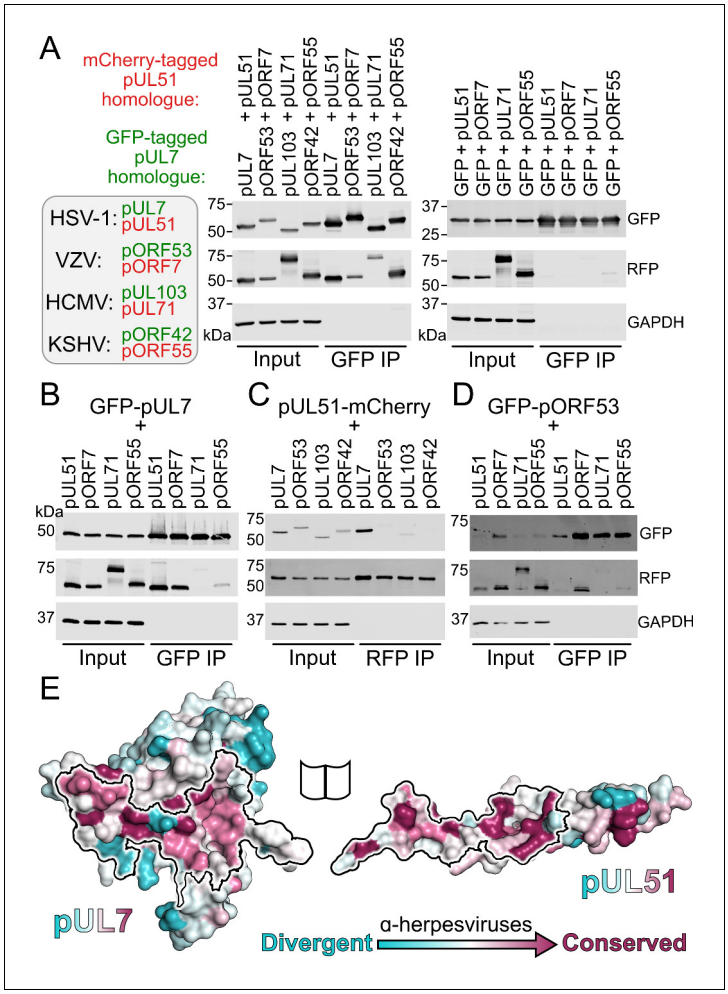

Figure 3. Conservation of the pUL7:pUL51 interaction across herpesviruses. (**A–D**) HEK 293 T cells were co-transfected with GFP-tagged pUL7 homologues from human herpesviruses, or with GFP alone, and with mCherry tagged pUL51 homologues. Cells were lysed 24 hr post-transfection and incubated with anti-GFP (**A, B, D**) or anti-RFP (**C**) resin to capture protein complexes before being subjected to SDS-PAGE and immunoblotting using the antibodies shown. All immunoblots are representative of at least two independent experiments performed by different scientists. (**A**) mCherry-tagged homologues of pUL51 are captured by GFP-pUL7 homologues, but not by GFP alone. (**B**) GFP-pUL7 co-precipitates with pUL51 (HSV-1) and pORF7 (VZV), but not with pUL71 (HCMV) or pORF55 (KSHV). (**C**) pUL51-mCherry co-precipitates with pUL7 but not with homologues from other herpesviruses. (**D**) The VZV pUL7 homologue pORF53 co-precipitates with VZV pORF7, but not with pUL51 homologues from other herpesviruses. (**E**) Molecular surfaces of the pUL7 and pUL51 core heterodimer, colored by residue conservation across the α-herpesviruses. Residues that mediate the pUL7:pUL51 interaction are outlined.

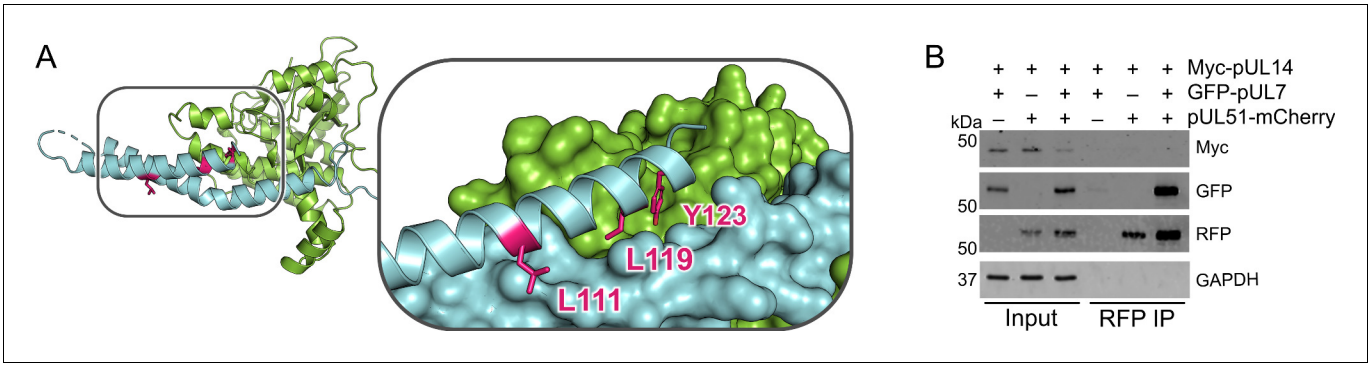

Figure 3—figure supplement 1. pUL51 does not co-precipitate pUL14 in uninfected cultured cells. (**A**) Core heterodimer of pUL7:pUL51 with residues required for the reported pUL51 and pUL14 (***Oda et al., 2016***) highlighted in pink. Inset shows pUL7 and the first helix of pUL51 as surfaces, and side chains of residues that were substituted with alanine in ***Oda et al., 2016*** are shown as sticks. (**B**) HEK 293 T cells were co-transfected with myc-tagged pUL14 from HSV-1 along with GFP-pUL7 and pUL51-mCherry, as shown. Co-immunoprecipitation of myc-pUL14 with pUL51-mCherry is not observed either in the presence or absence of pUL7. Image shown is representative of three independent experiments.

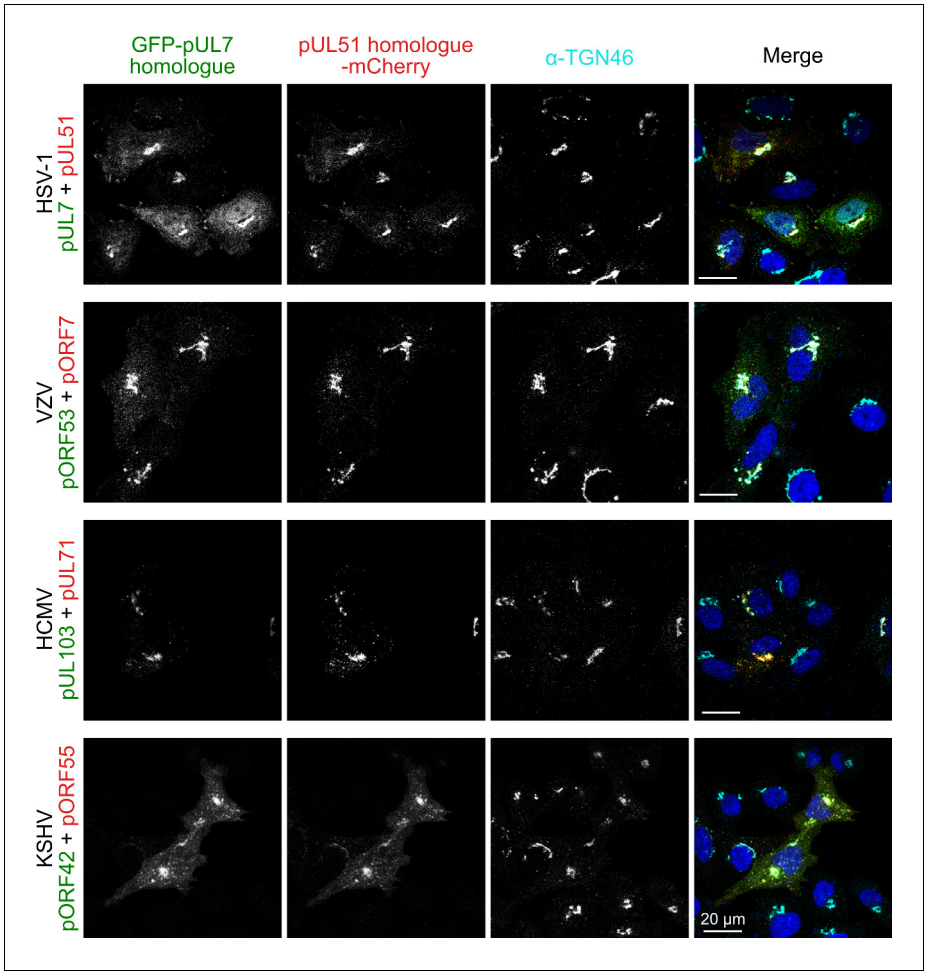

Figure 4. Co-localization of the pUL7:pUL51 complex with *trans*-Golgi membranes is conserved across human herpesviruses. HeLa cells were co-transfected with GFP-pUL7 and pUL51-mCherry, or with similarly-tagged homologues from VZV, HCMV and KSHV. Cells were fixed 24 hr post transfection and immunostained using the *trans*-Golgi marker protein TGN46 before imaging by confocal microscopy. Co-localization between the GFP, mCherry and far-red (TGN) fluorescence is observed in cells transfected with either HSV-1 pUL7:pUL51 or with the homologous complexes from VZV, HCMV and KSHV. HSV-1 pUL7 and pUL51 also co-localize with striated cell peripheral structures (focal adhesions, see ***Figure 4—figure supplement 1*** and ***Figure 4—figure supplement 2***). Images are representative of experiments performed in three cell lines (TERT-immortalized human foreskin fibroblasts, U2-OS osteosarcoma cells and HeLa cells) by two independent scientists.

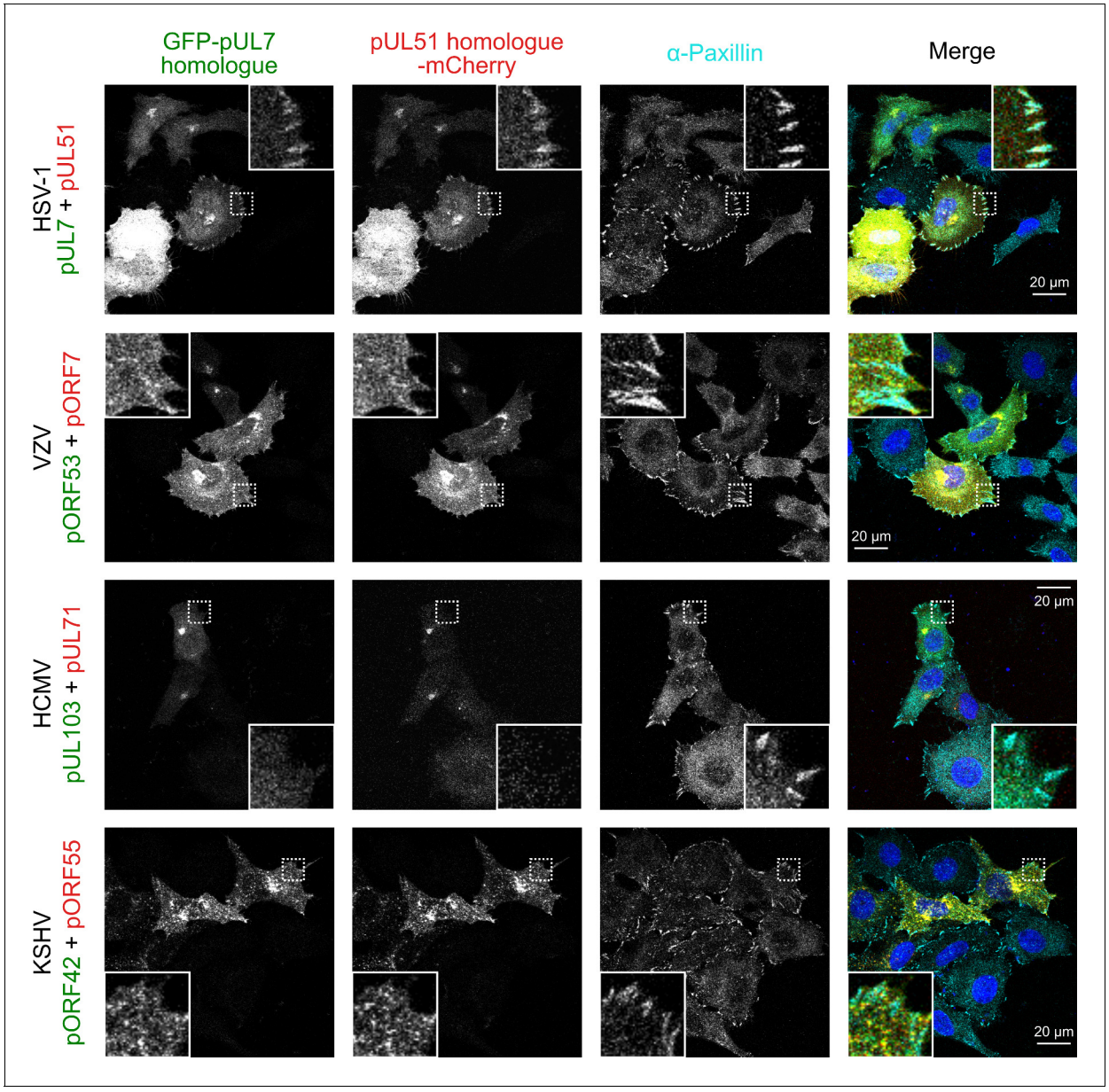

Figure 4—figure supplement 1. The pUL7:pUL51 complex from HSV-1 co-localizes with focal adhesion marker paxillin, but homologues from other human herpesviruses do not. HeLa cells were co-transfected with GFP-pUL7 and pUL51-mCherry, or with similarly-tagged homologues from VZV, HCMV and KSHV. Cells were fixed 24 hr post-transfection and immunostained for the focal adhesion marker protein paxillin before imaging by confocal microscopy. Co-localization between the GFP, mCherry and far-red (paxillin) fluorescence was only observed for cells transfected with HSV-1 pUL7-GFP and pUL51-mCherry. Images are representative of experiments performed in two cell lines (U2-OS osteosarcoma cells and HeLa cells).

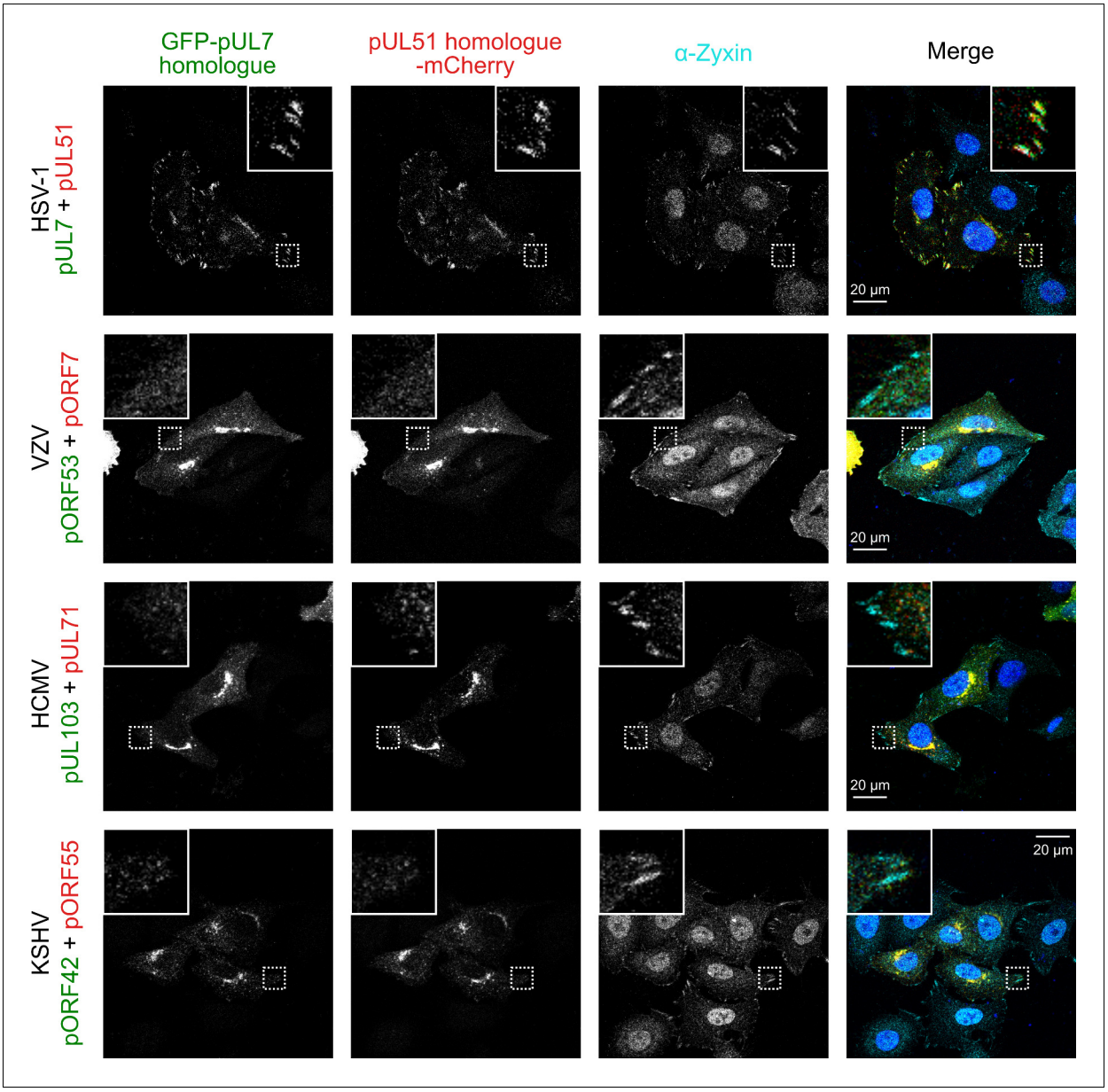

Figure 4—figure supplement 2. The pUL7:pUL51 complex from HSV-1 co-localizes with focal adhesion marker zyxin but homologues from other human herpesviruses do not. HeLa cells were co-transfected with GFP-pUL7 and pUL51-mCherry, or with similarly-tagged homologues from VZV, HCMV and KSHV. Cells were fixed 24 hr post-transfection and immunostained for the focal adhesion marker protein zyxin before imaging by confocal microscopy. Co-localization between the GFP, mCherry and far-red (zyxin) fluorescence was only observed for cells transfected with HSV-1 pUL7-GFP and pUL51-mCherry. Images are representative of experiments performed in three cell lines (TERT-immortalized human foreskin fibroblasts, U2-OS osteosarcoma cells and HeLa cells) by two independent scientists.

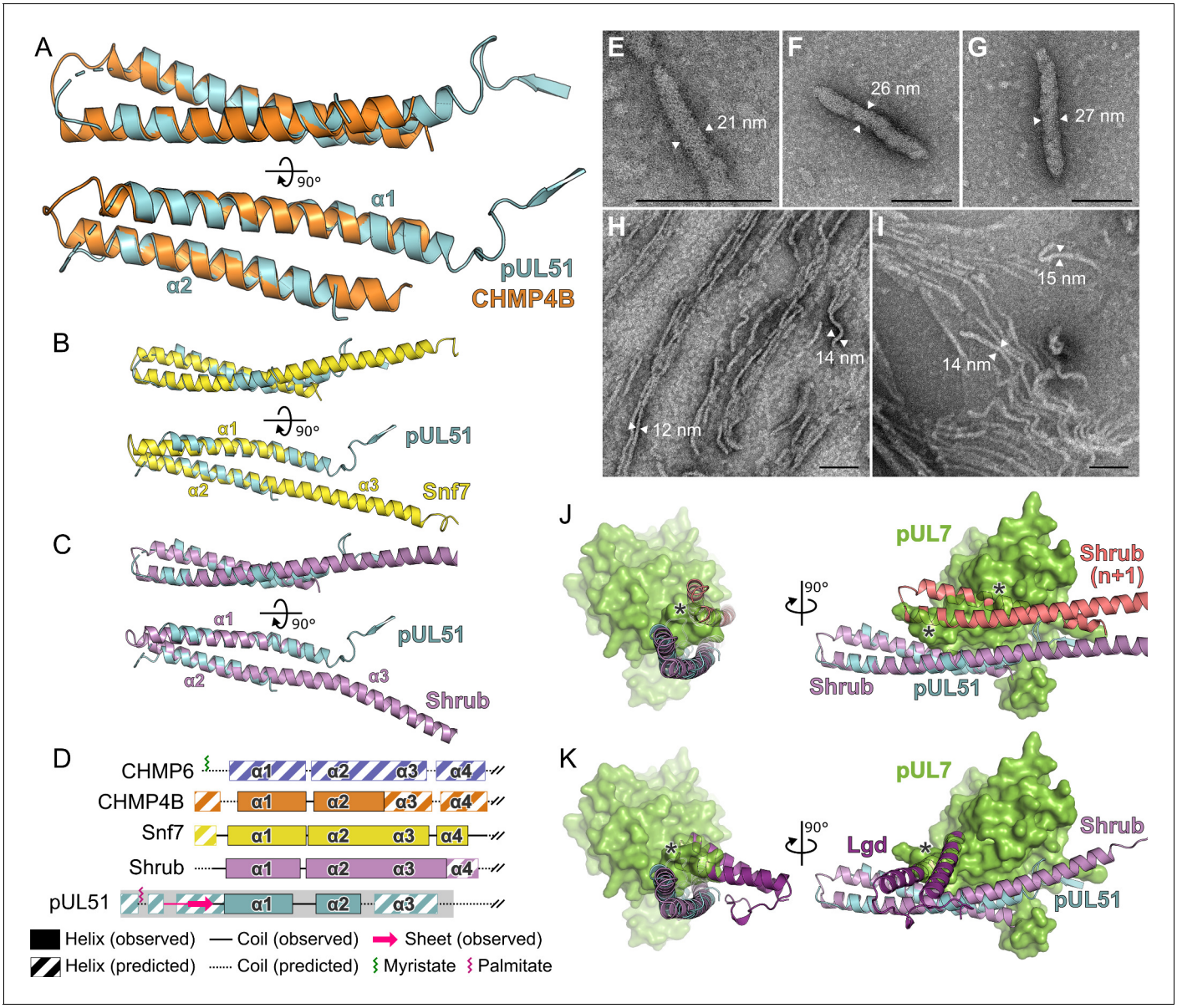

Figure 5. Structural similarity of HSV-1 pUL51 to cellular ESCRT-III proteins. (**A**) pUL51 (cyan) is shown superposed on the helical hairpin (conserved helices α1 and α2) of human CHMP4B (orange; PDB 4ABM) (***Martinelli et al., 2012***). (**B and C**) pUL51 (cyan) superposed on conserved helices α1 and α2 of CHMP4B homologues (**B**) yeast Snf7 (yellow; PDB 5FD7) (***Tang et al., 2015***) and (**C**) fly Shrub (violet; PDB 5J45) (***McMillan et al., 2016***). Note helices α2 and α3 of the ESCRT-III core domains of that Snf7 and Shrub are elongated and continuous in polymeric forms of these proteins (***Tang et al., 2015***; ***McMillan et al., 2016***). (**D**) Schematic representation of selected cellular ESCRT-III protein core domains and pUL51. Residues 1–150 of cellular ESCRT-III proteins and 1–190 of pUL51 are depicted. Secondary structure of crystal structures shown in panels **A–C** are in solid lines (coil) and solid boxes (helices). Predicted secondary structure (***Petersen et al., 2009***) outside these regions is shown as dotted lines (coil) and striped boxes (helices). The N-terminal region of pUL51 that forms a β-sheet with the pUL7 cloning tag, presumably an artefact of crystallization, and preceding residues are shown in pink. The region of pUL51 used for electron microscopy analysis is shaded in grey. Myristoylation (CHMP6) or palmitoylation (pUL51) sites are indicated by green and purple sticks, respectively. (**E–I**) Negative stain transmission electron microscopy images of pUL51 filaments. Scale bars, 100 nm. (**E–G**) Representative images of pUL51 proto-filaments formed when 100 μM pUL51(1–170) in 20 mM tris pH 8.5 was incubated on grids for 30 s before staining. (**H, I**) Representative images of pUL51 filaments formed when 10 μM pUL51(1–170) in 20 mM HEPES pH 7.5 was incubated on grids for 1–2 min before staining. (**J and K**) The pUL7:pUL51 core heterodimer is shown superposed onto (**J**) two subunits of the putative Shrub homopolymer (violet and pink; PDB 5J45) (***McMillan et al., 2016***), or (**K**) the complex of Shrub with the regulatory DM14-3 domain of Lgd (purple; PDB 5VO5) (***McMillan et al., 2017***). pUL7 is shown as a green molecular surface. Spatial overlap between pUL7 and (**J**) the second subunit of Shrub, or (**K**) the Lgd DM14-3 domain, is denoted by asterisks.

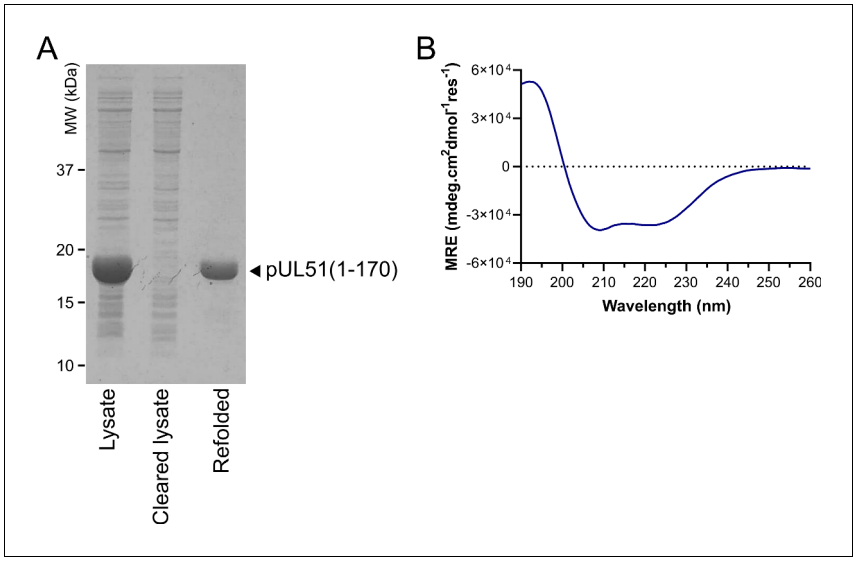

Figure 5—figure supplement 1. Purification of His-tagged pUL51(1-170). (**A**) Coomassie-stained SDS-PAGE analysis of His-pUL51(1–170) purification from inclusion bodies, showing depletion of insoluble pUL51 from the bacterial cell lysate by centrifugation and the purified sample after refolding. (**B**) Circular dichroism spectrum of His-pUL51(1–170). The spectrum is consistent with the pUL51 N-terminal region having a predominantly α-helical composition, as expected from the crystal structure and secondary structure predictions (***Figure 2***; ***Figure 1—figure supplement 2***). Decomposition of the spectrum using CDSSTR (as implemented by DichroWeb) gives an overall helical fraction of 0.8 (0.6 regular α-helix, 0.2 distorted α-helix) with a normalized root-mean-square deviation of 0.002 over 177 residues. MRE, mean residue ellipticity.